Journal of Luminescence 209 (2019) 316–320

Contents lists available at ScienceDirect

Journal of Luminescence

journal homepage: www.elsevier.com/locate/jlumin

TL properties of BaF_2:Ce phosphor for high gamma ray dosimetry

Kishor H. Gavhane[a,1], Mahesh S. Bhadane[a,1], Akash P. Jadhav[a], Bhushankumar J. Patil[b], Vasant N. Bhoraskar[a], Shailendra S. Dahiwale[a,*], Sanjay D. Dhole[a,*]

[a] Microtron Accelerator Laboratory, Department of Physics, Savitribai Phule Pune University, Pune 411007, India
[b] Department of Physics, Abasaheb Garware College, Pune 411007, India

ARTICLE INFO

Keywords:
Thermoluminescence
BaF_2
^{60}Co gamma source
Co-precipitation method

ABSTRACT

Powder sample of Cubic phase BaF_2:Ce phosphor was synthesized by chemical co-precipitation method and annealed at 500 °C for 2 h. The synthesized powder of BaF_2:Ce phosphor was characterized by XRD, which shows FCC structure with 30 nm crystallite size. TEM images show a cubic structure and FTIR contains the existence of F-Ba-F, C-H, C=C, and O-H bonds. Glow curve of the Thermoluminescence contains two major peaks, one at 175 °C and another at 275 °C. The intensity of the major dosimetric peak (175 °C) observed to be increased linearly from 1 Gy to 3 kGy for the doses of ^{60}Co gamma rays and then saturates. Overall, the new BaF_2:Ce phosphor shows good material properties for the high gamma dose measurement applications.

1. Introduction

Luminescence deals with the substances which absorb energy either in form of light, radiation, mechanical or something from an external source and subsequently emit energy in the form of visible light. Properties of luminescent phosphors can be tuned by adding impurity inside the host materials. Although, for tunability of such phosphors the impurities are significantly important in order to create defects; which should mainly produce the luminescence. As a result, thermoluminescence (TL) emission of the rare earth impurity phosphors is favorably affected, provided they are not producing the luminescence killing centers. The dopant is the main candidate to change the luminescence properties for different types of applications, such as white light LEDs [1], afterglow materials [2], fluorescent lamps [3], scintillators [4–6], and in dosimeters [6–9]. On the formation of phosphors as dosimetry, the doping of different impurities into host materials can retain a large number of defects. Some of the well-known dopants and host materials especially used for dosimeters are Dy in $CaSO_4$ [10] & CaF_2 [11], Mg-Ti & Mg-Cu-P in LiF [12], C in Al_2O_3 [13], Cu in $Li_2B_4O_7$ [14,15], and EuCe in $K_2Ca_2(SO_4)_3$ [16]. Such doping has enhanced the defects for the dosimetric application. This dopant can form more quantity of trapping centers to help to enhance the luminescence properties as well as dosimetric behavior. The dosimetric phosphors are classified into two basic types: (i) semiconductor phosphors (which are mostly applicable to light emitting devices) and (ii) insulator phosphors (graded phosphors). In case of TL, graded phosphors like insulator are the most important due to their dosimetric traps because it stores the radiation data for a longer time ($> 10^{-8}$ sec) than the shallow traps which cause abrupt radiation losses ($< 10^{-8}$ sec) [17].

As per the simple band model of TL, if the electron trap depth is more from conduction band and the frequency factor of the respective trap, then the probability of radiation loss with a period of time is very less. Hence, such electron traps are beneficial which produce dosimetric centers with sufficient trap depth [18]. Moreover, the glow curve temperature peak comes in the range of 170–300 °C which corresponds to the relatively deeper level traps (E = 0.75 – 1.25 eV) [19]. This allows one to have better properties of dosimetric trapping center and hence higher TL efficiency. In general, due to this fact, variation in the trapping levels (deeper level traps; far to CB) have more probabilities to use graded dosimeters (standard TLDs), and attributed to the applications such as medical dosimetry, personal and environmental monitoring, neutron dosimetry, space research, dating etc. [20–25]. Another factor of importance, *viz*. the homogeneous type of dosimeters are available that originates due to their own properties with a particular application. None the less due to wide band gap, some fluoride materials do address numerous interesting properties such as LiF as making for a low-temperature co-fired ceramic [26], CaF_2 as antibacterial agent [27], SrF_2 as energy transfer processes [28], and BaF_2 as scintillators [29] including the dosimetric applications indicate their strength.

Among them, the BaF_2 is a high Z material ($Z_{eff.}$ = 50.96) and also shows remarkable results in the field of luminescence [30–32]. From the last couple of decades, BaF_2 doped with rare earth impurities is used

* Corresponding authors.
E-mail addresses: ssd@physics.unipune.ac.in (S.S. Dahiwale), sanjay@physics.unipune.ac.in (S.D. Dhole).
[1] Kishor H. Gavhane and Mahesh S. Bhadane contributed equally to this work.

https://doi.org/10.1016/j.jlumin.2019.02.011
Received 6 June 2018; Received in revised form 4 February 2019; Accepted 6 February 2019
Available online 07 February 2019

as Thermoluminescence and Radioluminescence applications because it is very sensitive to ionizing radiations. Some undoped alkaline fluorides also show the TL spectra at low temperature [33]. Other than TL, BaF_2 shows good energy transfer process in scintillation decay and smart quality as a scintillation detector [34,35]. In addition mono-crystals of BaF_2 also used for investigating optical properties and new scintillation sensors in positron emission tomography [36]. However, the data scares in Thermoluminescence point of view. Recently, it is reported [37] that the Dy doped BaF_2 shows a quite good linear dose-response (i.e. 1 Gy to 3 kGy). On the other hand, some of the work reported in the literature [38,39] studied the inconsistent TL glow curve along with low-temperature peaks without any optimization process. As per the literature survey, there is a very little amount of work which has been done on BaF_2:Ce irradiated with X-rays, UV, and gamma rays as a function of wavelength, time [40]. Woztuwicz et al., has reported low-temperature TL study on BaF_2:Ce irradiated with X-rays and focused on details on the measurement of scintillation light yields and time profile [41]. But, as per our knowledge, very little of work has been carried out on TL dosimetry. Taking motivation from the work done till now, the present study is mainly focused on high gamma dose measurement at room temperature TL properties.

In the present work, we have synthesized BaF_2:Ce phosphor by co-precipitation method with different Ce molar concentration. The structural, morphological, and luminescent properties of Ce doped barium fluoride phosphor have been studied. To improve the TL dosimetric efficiency, phosphors are annealed and quenched at different temperatures with time variations and optimized for the efficient dosimetric phosphor. The glow curve of BaF_2:Ce (1 mol%), shows two dosimetric peaks at 175 °C and 275 °C. Here, the systematic study on optimization of temperature dependent TL properties was carried out. TL characteristics such as linear dose response, fading, and reproducibility have been studied for the application of radiation dosimetry.

2. Experimental

2.1. Sample preparation

The highly sensitive BaF_2:Ce phosphor was prepared by chemical co-precipitation method with the following reaction.

$$BaCl_2 + 2NH_4F \rightarrow BaF_2 + 2NH_4Cl$$

In a typical process, 5.71 gm of $BaCl_2$ and 1.74 gm of NH_4F was dissolved separately into 20 ml (99.9% pure, A.R Grade) and 30 ml double distilled water (DDW) with continuous stirring. Each solution was stirred up to 30 min in a natural atmosphere. After that, 1 mol% cerium oxide (CeO_2) (used as a dopant) from Sigma Aldrich was dissolved in $BaCl_2$ solution under continuous stirring and subsequently, 25 ml ethanol was added to it. Stoichiometric compositions of NH_4F solution was inserted drop by drop in the $BaCl_2$ solution under the continuous stirring condition. The reaction was continued further for another 2 h 30 min to generate precipitation. Finally, the precipitate was filtered out and dried at 120 °C for 5 h. This dried powder was then used for all the characterizations.

2.2. Characterization

X-ray diffraction (XRD) pattern was recorded using Brucker D-8 advanced powder instrument with Cu K_α radiation ($\lambda = 1.5406$ Å). Transmission electron microscopic images and selected area electron diffraction were taken on FEI Netherlands, Technai G^2 20 ultra twin microscope operating at 200 kV. TL glow curves were recorded using TLD reader (Model no. 1009I) with the heating rate (β) of 5 °C/s.

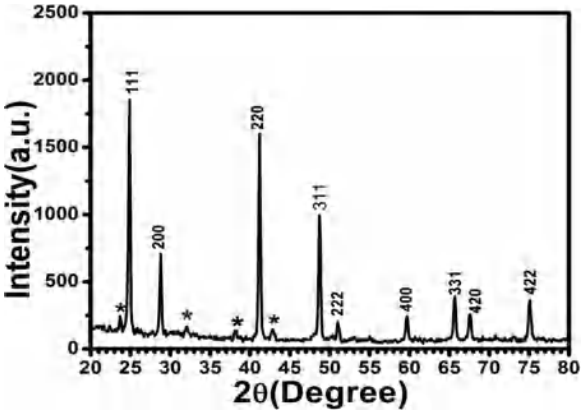

Fig. 1. X-ray diffraction pattern of cubic BaF_2:Ce phosphor.

3. Results and discussion

3.1. X-ray diffraction and EDS analysis

XRD pattern of BaF_2:Ce phosphor shown in Fig. 1 matches very well with the standard data available in JCPDS card (ICDD card no. 85-1342). The pattern indicates the cubic structure. The crystallite size determined by Scherrer's formula was found to be ~30 nm. XRD showed some '*hkl*' peaks at 24.9°, 28.8°, 41.2°, 48.7°, 51.0°, 59.6°, 65.6°, 67.5°, and 75.0° corresponding to (111), (200), (220), (311), (222), (400), (331), (420), and (422) planes respectively. Due to the small amount (1 mol%) of dopant, no peaks from impurities are observed. Some unidentified peaks observed in the XRD of BaF_2:Ce such as 23.8°, 32.1°, 38.2°, and 42.8° denoted as '*' are might be due to a small amount of un-reacted $BaCl_2$ remained into the sample which is well agreement with ICDD card number 74-0524 data file of $BaCl_2$.

The elemental analysis of BaF_2:Ce phosphor was done using EDS and the plot of the spectrum is shown in Fig. 2. The atomic percentage (%) of elements detected by EDX is shown in Table 1, which indicates that synthesized materials are in a stoichiometric amount.

3.2. TEM analysis

The size of nanoparticles and its morphology was made through high magnification and TEM which is an important technique in materials research [42]. Fig. 3 shows a typical TEM image of for synthesized BaF_2:Ce. The shape of the BaF_2:Ce nanoparticles indicates a cubic form and having the size of these cubes quite uniform. An average particle size of BaF_2:Ce phosphor is observed around ~ 99 nm. The SAED pattern of a selective BaF_2 phosphor (inset in Fig. 3.c) showed clear spots of a diffraction pattern revealing a single-crystal-like cubic structure.

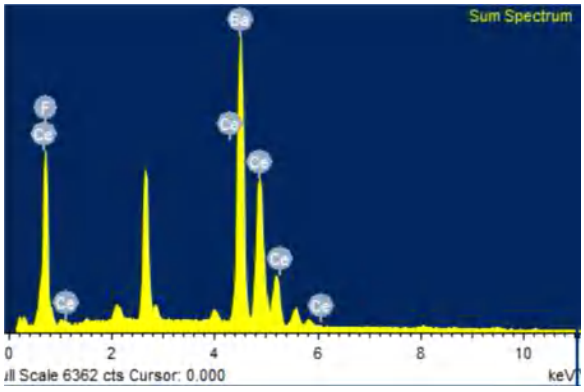

Fig. 2. EDS spectrum of BaF_2:Ce phosphor.

Table 1
Elemental composition of BaF_2:Ce.

Element	Atomic %
F	71.09
Ba	28.86
Ce	0.05
Total	100%

3.3. FTIR spectroscopy

The FTIR spectrum of BaF_2:Ce phosphor is shown in Fig. 4. It exhibits the presence of different bands at 1084, 832, and 735 cm^{-1} which correspond to F-Ba-F bands. It also reveals the presence of bands corresponding to F-anions. Moreover, some of the bands like C-H and C=C (i.e. at 1430 cm^{-1} and 1614 cm^{-1} respectively) shown in bending mode. The common strong prominent absorbance bands noted at 3230 cm^{-1} and 3450 cm^{-1} and can be assigned to the O–H bending vibrations of the residual water that is physically adsorbed onto the surface of the particles.

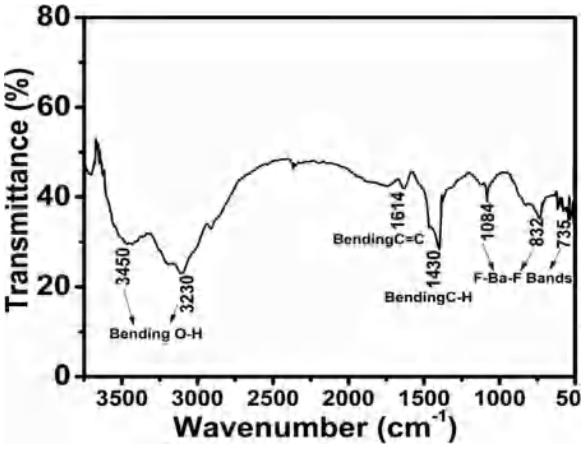

Fig. 4. FTIR spectrum of BaF_2:Ce phosphor.

3.4. Photoluminescence spectroscopy

PL emission spectra obtained by exciting the sample with UV light, is shown in Fig. 5. The emission spectra of Ce doped BaF_2 phosphor shows strong band at 345 nm which is excited by 280 nm wavelength. This is due to 5d-4f transmission of the Ce^{3+} and it shows the presence of Ce in the host BaF_2 sample.

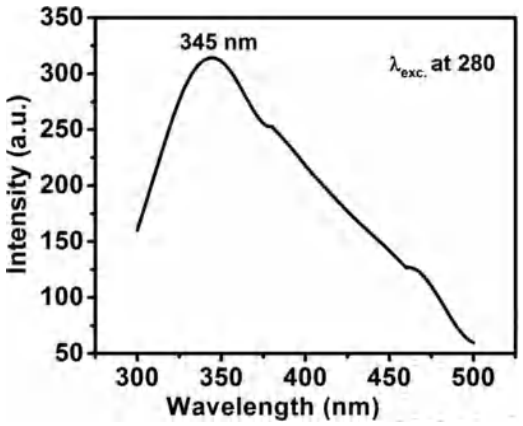

Fig. 5. Emission spectra of Ce doped BaF_2 phosphor. All spectra were recorded in the UV region.

3.5. Thermoluminescence properties

3.5.1. Glow curve and response curve

BaF_2 phosphor samples are doped with different concentrations of Ce (i.e. pristine, 0.5 mol%, 1 mol%, 1.5 mol%, and 2 mol%), to study the effect of Ce on the TL glow curve intensity and structure is shown in Fig. 6(a). Here, we took '5 mg' irradiated powder each time for TL spectra measurement and noticed that 1 mol% Ce doped BaF_2 showed a maximum intense glow. Other concentrations such as 0.5, 1.5, 2 mol% including pristine of BaF_2:Ce phosphor shows inconsistent and lower level glow temperature peaks. It may happen because, beyond the certain concentration, the luminescence efficiency starts falling with further increase of dopant concentration. So, we have chosen BaF_2:Ce 1 mol% phosphor as an optimized sample for further measurements. BaF_2:Ce 1 mol% phosphor was then annealed at 500 °C for different time intervals from 0.5 h to 4 h as shown in the Fig. 6(b) and 500 °C for 2 h samples give maximum intensity as compared to other time scale annealed phosphor.

Fig. 7 shows the optimized TL glow curves of the BaF_2:Ce phosphor exposed to gamma rays at a dose of 1 kGy. Optimization of the TL material is one of the ways to improve the efficiency, sensitivity, and dose storage capability. The TL properties exhibited by a phosphor strongly depend upon the kind of thermal annealing. In general, more defects are produced by quenching effect at the particular temperature (400–600 °C) facilitates the formation of defects levels leading to radiative transition, whereas quenching from the temperatures higher

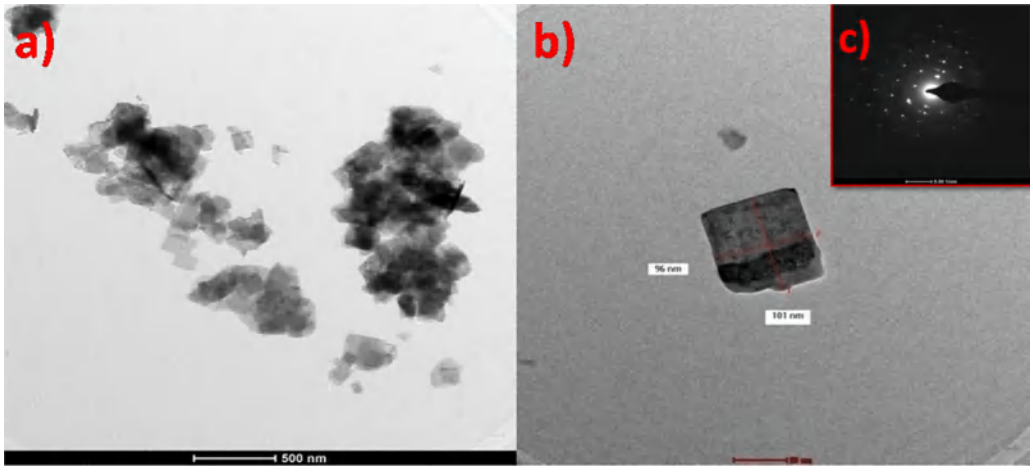

Fig. 3. TEM image of the cubic shape of BaF_2:Ce phosphor (a and b) and SAED pattern (c).

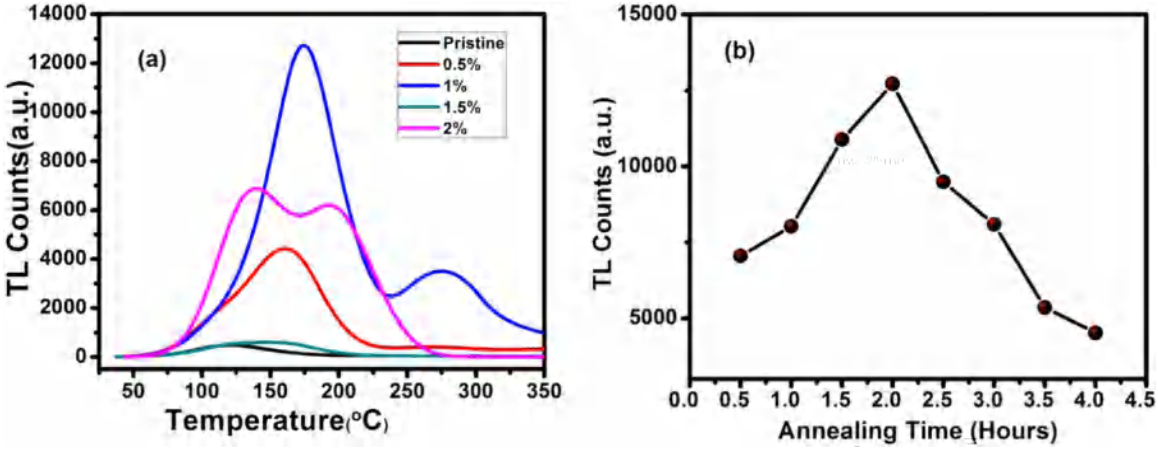

Fig. 6. Optimized of a glow curve of BaF_2:Ce (500 °C) phosphor irradiated a dose of 1 kGy gamma rays. (a) Different concentrations of 'Ce' dopant and (b) is 1 mol% of 500 °C annealing at different time scale rate (i.e. 0.5–4 h).

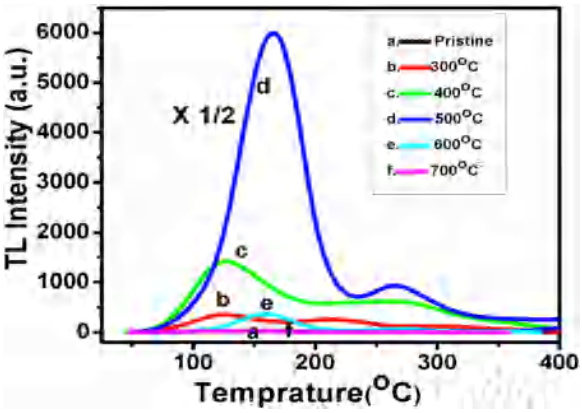

Fig. 7. Optimization glow curve of BaF_2:Ce phosphor irradiated with a dose of 1 kGy gamma rays at the different annealing temperature.

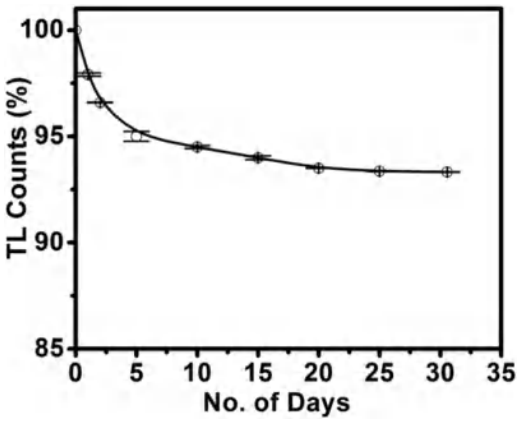

Fig. 9. The fading curve for BaF_2:Ce phosphor irradiated at 1 kGy of gamma dose.

than the 700 °C results into formation of defect levels leading to non-radiative transition. Herewith, the TL material BaF_2:Ce annealed at different temperatures from 300 °C to 700 °C in a step of 100 °C. Among all, 500 °C annealed BaF_2:Ce phosphor showed maximum intense glow peak. Therefore, BaF_2:Ce (1 mol%) phosphor annealed at 500 °C for 2 h was chosen as an optimized phosphor for further dosimetric studies.

TL glow curve for 500 °C, 2 h annealed BaF_2:Ce phosphor irradiated with different doses of gamma radiation from 1 Gy to 15 kGy is shown in Fig. 8(a). The glow curve mainly contains two dosimetric peaks at 175 °C and 275 °C. These two peaks correspond to two types of traps which are being activated within the particular temperature range with its own value of activation energy. It is observed that the TL peak intensity increases with an increase in dose up to 3 kGy and further saturates. However, there is no peak shifting in the peak position [43,44]. Fig. 8(b) shows the gamma dose-response curve for BaF_2:Ce phosphor. It is clearly observed from the figure that the dose-response exhibits

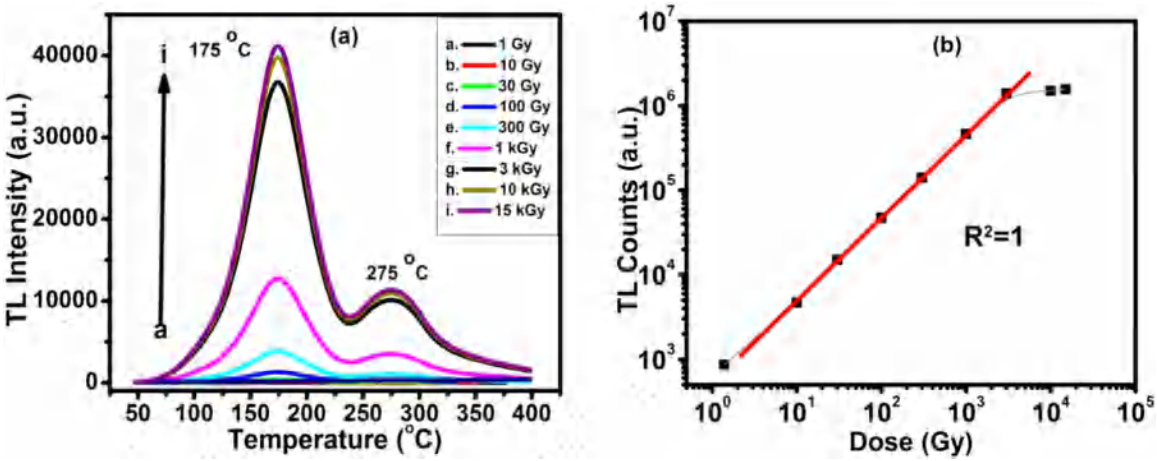

Fig. 8. (a) TL Glow curves of BaF_2:Ce phosphor irradiated at different doses of γ-rays from 1 Gy to 15 kGy. (b) TL response curve for BaF_2:Ce phosphor.

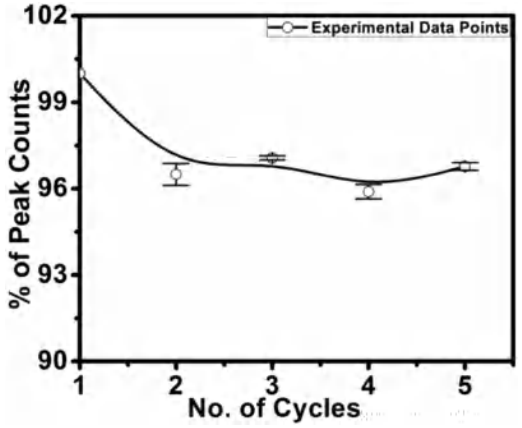

Fig. 10. Variation in % peak intensity of the TL curve of 5 mg BaF_2:Ce phosphor with the number of cycles.

linearity in the range from 1 Gy to 3 k Gy and further saturates with an increase in dose. The BaF_2:Ce phosphor shows the very good property as a linear dose range (Slope of R^2 fitting is ~1) and suggests to have one of the best materials for high gamma dose applications.

3.5.2. Fading and reproducibility

The fading is nothing but a rate of radiation loss per unit time. Sometimes shallow trap depth affected by environmental conditions and some phosphors loss absorbed dose after some time, that particular loss of radiation is known as fading. Ce doped BaF_2 phosphor which is irradiated at 1 kGy gamma dose revealed only 6.83% (± 0.381) fading up to one month. Fading data is plotted in Fig. 9, which concludes that the phosphor can be used as a dosimeter for various high gamma dose applications.

A dosimetric phosphor should not change during recurring annealing and repeated radiation exposures. Therefore, glow curve as well as the TL yield, should be stable all over complete storage of material, repeated irradiation, and reading. Here, TL plots were recorded for BaF_2:Ce phosphor, keeping the 5 mg sample constant for each irradiation 1 kGy of gamma dose. The remaining irradiated samples were annealed at 400 °C and repeated number of measurements under the constant irradiation and reading conditions. These procedures were carried out again and again at least 5 times. Accordingly, the constancy of the phosphor was obtained which is observed to be quite well for all the 5 sets and the result is shown in Fig. 10. For the justification of a good TL dosimetric material, sensitivity and efficiency of the phosphor should remain constant even after several numbers of repetitions of dose exposures and readouts. If this condition is satisfied, the TL material can be used for dosimetric applications and our result shows quite well constancy.

3.6. Conclusion

In conclusion, a luminescent phosphor of BaF_2:Ce has been successfully synthesized, by co-precipitation route. The structural study of BaF_2:Ce phosphor shows a cubic structure with average crystallite size 30 nm. TEM also confirms the square-cube like structure. The Thermoluminescence investigations and the optimized 500 °C annealed for 2 h BaF_2:Ce shows two peaks at 175 °C and 275 °C. The intensity of the glow peak was increase linearly with increasing dose from 1 Gy to 3 kGy. Different properties of TL including linear response, fading 6.83% for 2-month, and dose reproducibility are favourable results for BaF_2:Ce phosphor to be used as a high gamma dosimeter. This phosphor material may also be a promising candidate for both solid-state lighting and display devices.

Acknowledgment

One of the authors MSB is thankful to UGC, New Delhi, Govt. of India for awarding UGC-BSR fellowship.

References

[1] C. Qin, Y. Huang, L. Shi, G. Chen, X. Qiao, H.J. Seo, J. Phys. D: Appl. Phys. 42 (2009) 185105.
[2] Z. Xia, A. Meijerink, Chem. Soc. Rev. 46 (2017) 275.
[3] R. Purbia, S. Paria, Biosens. Bioelectron. 79 (2016) 467.
[4] K. Takagi, T. Fukazawa, Appl. Phys. Lett. 42 (1983) 1.
[5] Li Yang, Y. Wan, H. Weng, Y. Huang, C. Chen, H. Jin Seo, J. Phys. D: Appl. Phys. 49 (2016) 325303.
[6] F. Nakamura, T. Kato, G. Okada, N. Kawaguchi, K. Fukuda, T. Yanagida, Ceram. Int. 43 (2017) 604.
[7] M.S. Bhadane, S.S. Dahiwale, K.R. Sature, B.J. Patil, N.T. Mandlik, V.N. Bhoraskar, S.D. Dhole, J. Alloy. Compd. 695 (2017) 1918.
[8] L.C. Oliveira, O. Baffa, J. Lumin. 181 (2017) 171.
[9] A.S. Pradhan, Radiat. Prot. Dosim. 1 (3) (1981) 153.
[10] A.R. Lakshmanan, M.T. Jose, O. Annalakshmi, Radiat. Prot. Dosim. 132 (1) (2008) 42.
[11] A.N. Yazici, R. Chen, S. Solak, Z. Yegingil, J. Phys. D: Appl. Phys. 35 (2002) 2526.
[12] P. Bilski, Radiat. Prot. Dosim. 100 (2002) 199.
[13] M.F. Ahmed, E. Schnell, S. Ahmad, E.G. Yukihara, Phys. Med. Biol. 61 (2016) 7484.
[14] J.K. Srivastava, S.J. Supe, J. Phys. D: Appl. Phys. 22 (1989) 1537.
[15] B. Tiwari, N.S. Rawat, D.G. Desai, S.G. Singh, M. Tyagi, P. Ratna, S.C. Gadkari, M.S. Kulkarni, J. Lumin. 130 (2010) 2076.
[16] B.J. Patil, M.S. Bhadane, N.T. Mandlik, S.S. Dahiwale, M.S. Kulkarni, B.C. Bhatt, V.N. Bhoraskar, S.D. Dhole, AIP Conf. Proc. 1665 (2015) 050109.
[17] A.J.J. Bos, Rad. Meas. 41 (2007) S45.
[18] R. Chen, S.W.S. McKeever, Theory of Thermoluminescence and Related Phenomena, World Scientific, Singapore, 1997.
[19] AIOP, Soviet Physics Solid State 18 American Institute of Physics, California, 1976.
[20] T. Kron, Radiat. Prot. Dosim. 85 (1999) 333.
[21] B.C. Bhatt, M.S. Kulkarni, Int. J. Lumin. Appl. 3 (2013) 6.
[22] T. Katona, M. Osvay, A. Kelemen, M. Prokic, Radiat. Meas. 45 (2010) 707.
[23] M.S. Bhadane, N.T. Mandlik, B.J. Patil, S.S. Dahiwale, K.R. Sature, V.N. Bhoraskar, S.D. Dhole, J. Lumin. 170 (2016) 226.
[24] G.F. Mackay, T. Thomson, M. Ieee, A. Ng, N. Sultan, S.M. Beee, IEEE Trans. Nucl. Sci. 44 (1997) 2048.
[25] A.K. Singhvi, Y.P. Sharma, D.P. Agrawal, Nature 295 (1982) 313.
[26] Nuo-Xin Xu, Jue-Hui Zhou, H. Yang, Qi-Long Zhang, Min-Jia Wang, L. Hu, Ceram. Int. 40 (2014) 15191.
[27] W.A. Bala, V.S. Benitha, K. Jeyasubramanian, G.S. Hikku, P. Sankar, S.V. Kuma, J. Fluor. Chem. 193 (2017) 38.
[28] M.Y.A. Yagoub, H.C. Swart, P. Bergman, E. Coetsee, AIP Adv. 6 (2016) 02504.
[29] John B. Czirr, Edward Catalano, Nucl. Instrum. Methods 143 (1977) 487.
[30] S. Hou, Y. Xing, X. Liu, Y. Zou, B. Liu, X. Sun, Cryst. Eng. Comm. 12 (2010) 1945.
[31] N. Abe, Y. Yokota, T. Yanagida, J. Pejchal, F. Nara, N. Kawaguchi, K. Fukuda, M. Nikl, A. Yoshikawa, Jpn. J. Appl. Phys. 49 (2010) 022601.
[32] G. De, W. Qin, J. Zhang, J. Zhang, Y. Wang, C. Cao, Y. Cui, J. Solid State Chem. 179 (2006) 955.
[33] Principle of Thermoluminescence, Munish Kumar, BARC Mumbai.
[34] R. Vissert, P. Dorenbost, C.W.E. Eijkt, H.W. Hartogt, J. Phys. Condens. Matter 4 (1992) 8801–8812.
[35] C. AGODI, et al., Nucl. Instrum. Methods A269 (1988) 595.
[36] A.A. Demidenko, et al., Opt. Mater. 32 (2010) 1291.
[37] M.S. Bhadane, S.S. Dahiwale, V.N. Bhoraskar, S.D. Dhole, AIP Conf. Proc. 1731 (2016) 050149.
[38] G.M. Ferraz, M. Matsuoka, S. Watanabe, C.M. sunta, G.V.S.G. Acharyalu, R.V. Srikantaiah, Radiat. Eff. Defects Solids 154 (2001) 3.
[39] C. Shi, Z. Xie, J. Deng, Y. Dong, X. Yang, Y. Hu, Y. Tian, Y. Kan, J. Electron Spectrosc. Relat. Phenom. 79 (1996) 87.
[40] R. Vissert, et al., J. Phys. Condens. Matter 5 (1993) 1659.
[41] Andrzej J. Wojtowicz, et al., J. Phys. Condens. Matter 12 (2000) 4097.
[42] J. Geng, F. Jiang, Q. Lu, J.-Jie Zhu, Cryst. Eng. Comm. 13 (2011) 2758.
[43] C. Furetta, Handbook of Thermoluminescence, World Scientific, Singapore, 2010.
[44] Numan Salah, P.D. Sahare, Radiat. Eff. Defects Solids 159 (2004) 321.